Preparation of an $Li_{0.7}Ni_{0.8}Co_{0.2}O_2$ Electrode Material From a New Li–Co–Ni Mixed-Citrate Precursor

Yodalgis Mosqueda,[a] Eduardo Pérez-Cappe,[b] Pilar Aranda,[c] and Eduardo Ruiz-Hitzky*[c]

Keywords: Citrates / Electrode materials / Lithium batteries / Mixed-valent compounds / Oxides

A new chemical route to prepare the mixed oxide $Li_{0.7}Ni_{0.8}Co_{0.2}O_2$, which is a member of the well-known Li-Ni-Co-O family that is of interest as an electrode material for rechargeable lithium batteries, from a mixed citrate is reported. In a first step the new citrate $(NH_4)_3LiNi_{0.8}Co_{0.2}(C_6H_5O_7)_2$, is synthesized, which, after thermal decomposition, gives the layered mixed-oxide phase $Li_{0.7}Ni_{0.8}Co_{0.2}O_2$. This oxide has been characterized by chemical analysis, XRD, FTIR, SEM, and DTA, revealing an "ideal" trigonal α-$NaFeO_2$ type structure with a well-ordered distribution of Li and Ni ions in different lattices. Thermoelectric power and four-point electrical conductivity measurements indicate a nonactivated conductivity mechanism of a small polaron. The $Li_{0.7}Ni_{0.8}Co_{0.2}O_2$ compound prepared by this so-called "citrate route" has a better reversibility of Li-insertion in charge–discharge cycles than related phases reported previously.

Introduction

Among the $LiMO_2$ (M = V, Cr, Mn, Co, Ni) series, the $Li_x(Ni_{1-y}Co_y)_{1-x}O_2$ family shows structures based on either cubic close packed (fcc) or distorted (fcc) oxygen lattices.[1–3] These families of oxides exhibit very interesting physical and electrochemical properties that have made most of them applicable as positive electrodes in high-energy-density batteries.[4–8] The $Li_x(Ni_{1-y}Co_y)_{1-x}O_2$ system exhibits several advantageous properties in comparison to the $LiNiO_2$ and $LiCoO_2$ end members, such as higher capacity, lower material cost, better thermal stability, and superior rechargeable performance.[9–11] One of the key requirements to obtain a good electrode material within this family of compounds is to reach a good cationic order of Ni and Li ions in different structural sites. However, many authors have reported the presence of divalent nickel ions (r = 0.68 Å) at the lithium sites (r = 0.74 Å) in the nickel-rich phases because this element in its trivalent oxidation state is relatively unstable and, due to its small ionic size (r = 0.56 Å) fits better in the lithium octahedral position.[12–14] This can be seen by XRD and IR spectroscopy. In this way, strong overlap in the (006)/(012) and (018)/(110) couples of diffraction lines, as well as a (003)/(104) integrated intensity ratio lower than 1.2, indicate the presence of cationic disorder.[12,13] Moreover, the characteristic IR pattern in oxides with well-ordered cationic distribution, which consists of the presence of two well-individualized IR characteristic regions for the vibration modes of LiO_6 (300–200 cm^{-1}) and $M^{3+}O_6$ (650–400 cm^{-1}) sites, is lost.[15,16] When the lithium ions surrounding the nickel divalent ions are preferentially deintercalated, the oxidation process of extra nickel ions, i.e. from the divalent (r = 0.68 Å) to the trivalent state (r = 0.56 Å), takes place. On reversing polarity in the charge–discharge cycles, these lithium ions can no longer fit back into their sites due to octahedral distortion, and therefore the electrochemical cyclability is limited.[12,17,18]

Taking into account the above observations, one of the strategies for preparing materials with better cycling properties has been directed towards new routes of synthesis to produce trigonal ($R\bar{3}m$) Ni-rich phases with an ordered distribution of Li^+ and M^{3+} ions in the octahedral sites. Synthetic methods that lead to small-particle-size materials are also of interest because they favor the ionic and electronic diffusion in the cathode material intergrain frontiers, as well as the overpotential decrease of the ionic transfer across the cathode/electrolyte interface.[19,20] Chemical methods involving salts after precipitation and convenient thermal treatments have been the strategies for the preparation of small-particle-size oxides. In this way, the so-called citrate method has been employed in the preparation of multicomponent oxides (perovskites, spinels, ferrites, etc.) to produce materials with a high chemical homogeneity and small particle size.[21–30] This method involves the precipitation of citrate salts at controlled pH and concentration ratio of the involved ions, followed by their thermal decomposition. The Pechini process[26] for the synthesis of mixed oxides is one of the different reported pathways in which polyhydroxy alcohols are used to produce the esterification of

[a] Department of Chemistry, Orient University, Santiago de Cuba, Cuba
[b] Laboratory of Solid State Ionics, IMRE Havana University, Havana, Cuba
[c] Instituto de Ciencia de Materiales de Madrid, Cantoblanco 28049, Madrid, Spain
E-mail: eduardo@icmm.csic.es
Supporting information for this article is available on the WWW under http://www.eurjic.org or from the author.

  DOI: 10.1002/ejic.200400383

complex mixtures of citrates to give a polymeric resin, which is decomposed above 400 °C.[21,23–26] However, the formation of a dense and rigid resin intermediate of citric acid and ethylene glycol, which leads to crystallite agglomeration during pyrolysis, has been found to be a critical problem of this approach.[25] A modified Pechini method has been reported recently by Julien et al.,[30] in which a gel precursor is prepared by addition of citric acid to a mixture of the metal acetates followed by heating at 800 °C to obtain the micro-sized $LiNi_{0.6}Co_{0.4}O_2$ phase. Alternative routes[27–30] are based on the higher solubility of the citrate salts in ethanol vs. water, as reported by Zhecheva and coworkers[29] for the preparation of $LiCoO_2$ powders with small particle size. These authors showed that the chelating ability of citric acid, and therefore its ability to form complexes with metal ions, is highly dependent on the ions' concentration. Thus, concentrated lithium-cobalt-citrate solutions (1:1:2, Li:Co:citric acid) lead to the formation of a homogeneous $(NH_4)_3LiCo(C_6H_5O_7)_2$ citrate. The thermal decomposition of this amorphous citrate yields a $LiCoO_2$ phase with an "ideal" trigonal α-$NaFeO_2$-type structure.[29]

Although the method employed by Zhecheva et al.[29] is efficient for the preparation of lithium cobalt oxides, there is no evidence of its application to systems involving other metal such as nickel, or when a substitution of cobalt by nickel must take place. The aim of the present work is to extend Zhecheva's method[29] to the synthesis of $LiNi_{0.8}Co_{0.2}O_2$ by using, in this case, a new precursor consisting of a mixed nickel-cobalt citrate of appropriate stoichiometry. We intend to optimize the synthesis conditions to reach a well-defined crystalline phase of the mixed citrate that could produce the ideal trigonal Li-Co-Ni oxide (rich in nickel) by a new chemical route followed by thermal decomposition. As is reported below, the resulting oxide has a $Li_{0.7}Ni_{0.8}Co_{0.2}O_2$ composition whose structural and electrochemical features are studied in comparison with the phase of similar composition ($Li_{0.8}Ni_{0.8}Co_{0.2}O_2$) prepared by a ceramic method.

Results and Discussion

Preparation and Structural Characterization of the Precursor Citrate and the $Li_{0.7}Ni_{0.8}Co_{0.2}O_2$ Phase

During the preparation of the precursors of the Li-Co-Ni mixed oxides we observed that attempts to prepare the mixed citrates of a selected stoichiometry in the presence of lithium salts always resulted in mixtures of amorphous and crystalline Li-Co and Li-Ni phases, except when the pH and the concentration of the solutions were strictly controlled. Therefore, based on the experimental results of Zhecheva et al.[29] applied to lithium–transition metal (Co or Ni) citrate single-phase preparations, we estimated what would be the optimum pH value to obtain the Li-Co-Ni tridentate citrate as a single phase with a 1:1:2 Li:(Co-Ni):citrate ratio. The variation of the concentration of citrate (Cit) species vs. pH (Figure 1) is obtained by solving the three equilibrium equations of citric acid dissociation in water.[31]

$$H_3Cit\ (aq) \rightleftharpoons H_2Cit^-\ (aq) + H^+\ (aq);\ K_a = 8.4\times10^{-4} \quad (1)$$

$$H_2Cit^-\ (aq) \rightleftharpoons HCit^{2-}\ (aq) + H^+\ (aq);\ K_a = 1.8\times10^{-5} \quad (2)$$

$$HCit^{2-}\ (aq) \rightleftharpoons Cit^{3-}\ (aq) + H^+\ (aq);\ K_a = 4\times10^{-6} \quad (3)$$

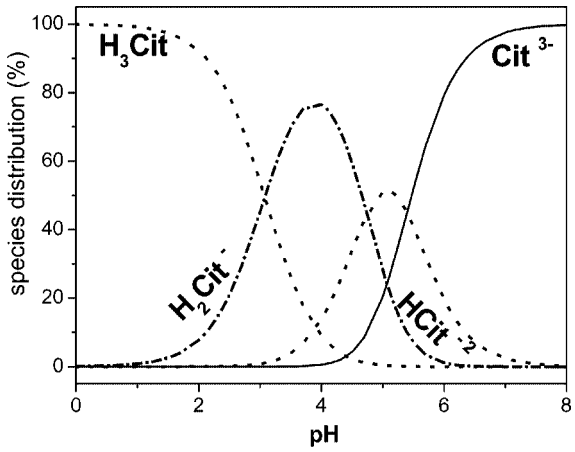

Figure 1. Phase diagram of citric acid species as a function of pH (calculated for a total citric acid concentration of 1 mol L^{-1}).

The distribution diagram of equilibrium species for citric acid shows that the Cit^{3-} species predominate around pH 7. To favor the presence of such species it is necessary to increase the pH, which in our case is achieved by adding the Li^+ ions as carbonate and, finally, aqueous ammonia solution to adjust to pH 7. Under these conditions Cit^{3-}, Li^+, Co^{2+}, Ni^{2+}, and NH_4^+ species are present, thus making possible the precipitation of the mixed citrate containing Li^+ and NH_4^+ ions, which act as counterions as with other reported ammonium metal citrates, such as $(NH_4)_4M(C_6H_5O_7)_2$ (M = Co, Zn, and Cu), studied by Zhecheva,[29] Swanson,[32] and Both,[33] respectively.

The mixed citrate $(NH_4)_3LiNi_{0.8}Co_{0.8}(C_6H_5O_7)_2$ obtained at pH 7 (see Experimental Section) precipitates as a blue-green solid when the resulting solution is dried. The elemental analysis (CHN) of the solid (C 28.40, N 9.19, H 4.12) is in good agreement with the calculated values (C 28.93, N 8.51, H 4.42). The STEM-EDX analysis of this sample for different particles of the solid shows Ni/Co, O/Ni, O/Co, and O/C atomic ratios of about 3.79, 4.56, 18.90, and 1.53, respectively, which indicate good homogeneity of the sample compositions.

The formation of a citrate salt is clearly revealed by IR spectroscopy (Figure 2) as the characteristic vibration bands of the carboxylic groups of the citric acid at 1740 cm^{-1} and 1690 cm^{-1} ($\nu_{C=O}$), 1420 cm^{-1} ($\nu_{CO} + \delta_{OH}$ in plane), and 930 cm^{-1} (δ_{OH} out plane) are replaced by the two characteristic antisymmetric and symmetric stretching vibration bands of carboxylate groups at 1576 cm^{-1} and 1385 cm^{-1}, respectively.[29,34] It is well known that the position and separation between ν_{as} and ν_s stretching vibrations of COO^- can be used to establish the coordination mode of the carboxylate anions around the metal ion.[35–37] The presence of the band assigned to the symmetric vibration

mode below 1400 cm^{-1} – it appears at 1385 cm^{-1} in the citrate synthesized here – suggests the coordination of the carboxylate as a bidentate ligand. The large band centered at 3190 cm^{-1} (Figure 2) can be assigned to the ν_{OH} stretching vibrations of perturbed 2-hydroxy groups, thus indicating the participation of such hydroxyls in the metal coordination. The bands at 1190 cm^{-1} and 1138 cm^{-1} correspond to the ν_{CO} stretching vibration modes of these tertiary alcohol groups.[34]

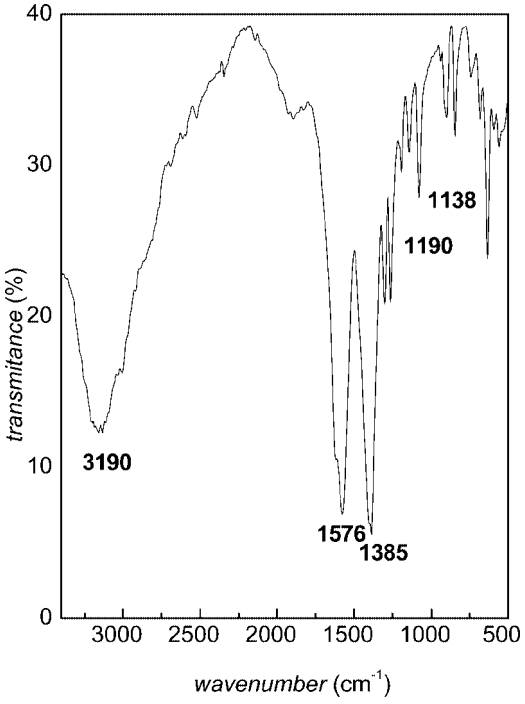

Figure 2. IR spectrum of the citrate $(NH_4)_3LiNi_{0.8}Co_{0.2}(C_6H_5O_7)_2$.

Figure 3 shows the XRD patterns of the mixed Li-Co-Ni citrate obtained at pH 7 (considered as the optimal acidity conditions) and another citrate obtained at pH 6. This latter solid exhibits a poor diffractogram, suggesting the presence of the citrate together with other phases, including amorphous materials. It is important to remark that thermal decomposition of both citrates results in different crystalline Li-Ni-Co mixed oxides with rhombohedral symmetry ($R\bar{3}m$).

The XRD patterns (Figure 3 c and d) are similar to those reported in the literature for $Li_{1-x}[Ni_{(x-y)}Ni_x]Co_{1-y}O_2$,[1–3,7,8,10,12,13] but a clear splitting of the (006) and (012) reflections as well as the (018) and (110) diffraction lines is observed for the oxide obtained from the citrate prepared at pH 7. This observation indicates that the corresponding mixed oxide has an α-$NaFeO_2$-type structure with a better ordered cationic distribution[12,13] than the oxide prepared from the citrate obtained at pH 6. The presence of NiO and Co_3O_4 phases that could take part in the resulting product can be discarded as their more intense XRD diffraction peaks do not appear in the patterns. Some of them could be overlapped by the most intense signals of the $Li_{0.7}Ni_{0.8}Co_{0.2}O_2$ mixed oxide but the other reflections are not detected in the background.

The XRD profiles of the ordered Li-Ni-Co mixed oxide as well as its new citrate precursor (pH 7) were indexed with the CELREF V3 computer program.[38] The unit-cell parameters in the hexagonal system (space Group: $R\bar{3}m$) are a = 0.2841 and c = 1.4070 nm, $\alpha = \gamma = 90°$, $\beta = 120°$ (calculated from the structural data in Table S1 in the Supporting Information). These parameters are not far from those of the $LiNi_{0.8}Co_{0.2}O_2$ oxide prepared by a ceramic route (a = 0.2867, c = 0.1416 nm, $\alpha = \gamma = 90°$, $\beta = 120°$ by Rougier[12] and a = 0.2862, b = 0.1412 nm, $\alpha = \gamma = 90°$, β

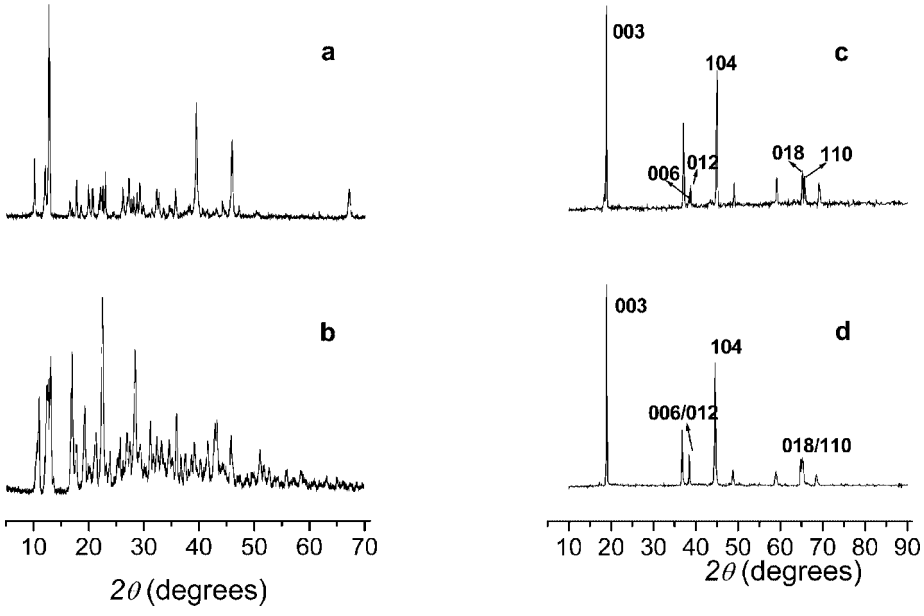

Figure 3. XRD patterns of the Li-Ni-Co citrate precursors obtained in this work at pH 7 (a) and pH 6 (b), and of the mixed Li-Ni-Co oxides obtained by thermal decomposition at 750 °C from the corresponding citrate prepared at pH 7 (c) and pH 6 (d).

= 120° in this work) or from those of $LiNi_{0.6}Co_{0.4}O_2$ reported by Julen et al.[30] by a sol-gel route (a = 0.2839, c = 0.1409 nm, $\alpha = \gamma = 90°$, $\beta = 120°$). For the precursor (citrate synthesized at pH 7) the unit-cell parameters in the monoclinic system ($P2_1/m$ space group) are a = 0.8839, b = 1.3768, c = 0.9057 nm, $\beta = 114.9°$ (powder X-ray diffraction data given in Table S2 in the Supporting Information).

The DTA and TG curves (Figure 4) of the citrate prepared at pH 7 show an endothermic peak at 140 °C, which is accompanied by a weight loss that was assigned to a first NH_3 loss according to TG/MS results (see Figure 1 in the Supporting Information). The complex endothermic peak observed between 170 °C and 240 °C accompanied by the second weight loss was assigned to loss of the residual NH_3 molecules and also the well known transformation of citrate $(C_6H_5O_7)^{3-}$ into *cis*-aconitate $(C_6H_3O_6)^{3-}$ and a water molecule.[21,25,29] Above 300 °C several exothermic processes take place accompanied by drastic weight losses due to the vigorous combustion reactions of the residual organic matter. The total weight loss for $(NH_4)_3LiNi_{0.8}Co_{0.2}(C_6H_5O_7)_2$ is about 82%, which agrees well with the calculated values for a final product of composition $LiNi_{0.8}Co_{0.2}O_2$ (80.5%).

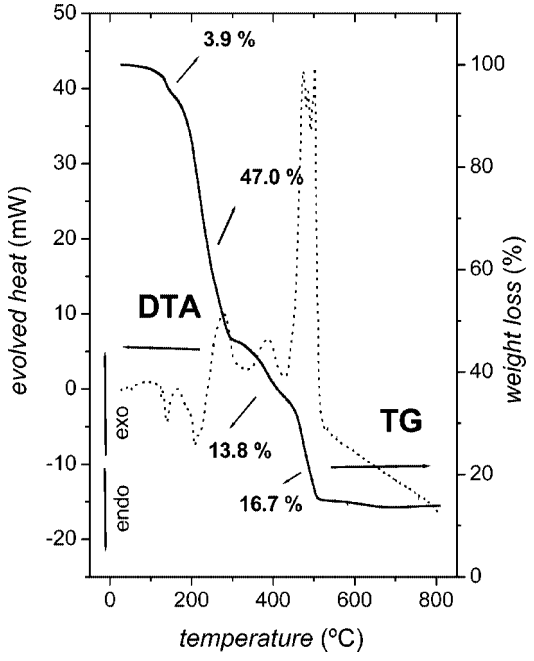

Figure 4. TG and DTA curves of the citrate $(NH_4)_3LiNi_{0.8}Co_{0.2}(C_6H_5O_7)_2$ heated in air.

The thermal evolution of the citrate synthesized at pH 7 was also followed by XRD with the objective to determine at what temperature this precursor is transformed into the lamellar mixed oxide with trigonal structure. Figure 5 shows that the citrate precursor gives the Li-Ni-Co-O-phase at 750 °C.

The citrate thermal decomposition at 750 °C for 30 hours gives a well-ordered $Li_xNi_{0.8}Co_{0.2}O_2$ material of composition 4.98% Li, 47.91% Ni, and 12.16% Co (see analytical data in Table S3 in the Supporting Information) that fits well with the ideal $Li_{0.7}Ni_{0.8}Co_{0.2}O_2$ phase (Li 5.08%, Ni

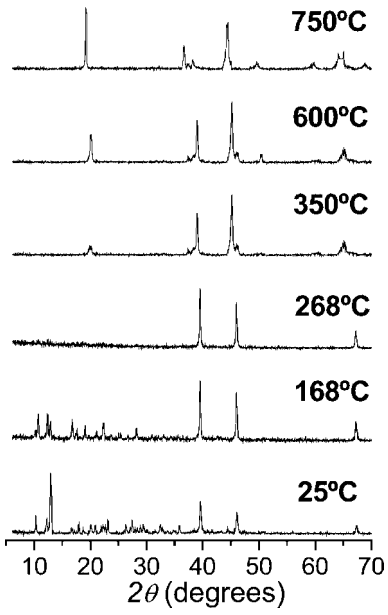

Figure 5. Evolution of the XRD patterns with temperature of the $(NH_4)_3LiNi_{0.8}Co_{0.2}(C_6H_5O_7)_2$ citrate precursor until transformation into the trigonal Li-Ni-Co-O mixed-oxide phase at 750 °C.

49.12%, Co 12.33%). From iodometric titration we deduced a mean oxidation state of +3 for both cobalt and nickel, i.e. Co^{III} and Ni^{III}. This result indicates that the loss of Li^+ does not lead to the formation of Ni^{2+} ions as some authors have proposed.[39] Moreover, in the present case the loss of Li^+ provokes the oxidation of Ni^{3+} and Co^{3+} to the +4 oxidation state, as will be discussed later in relation to the electrical characterization of the mixed oxide. The high temperature used during the citrate–oxide transformations could be responsible for the loss of lithium from the solids.

Figure 6 shows the IR spectrum of the $Li_{0.7}Ni_{0.8}Co_{0.2}O_2$ phase in the 200 to 800 cm^{-1} region. As observed in related Li-Co-Ni mixed oxides, the number of resolved IR bands (4 bands: 2 A_{2U} and 2 E_U) corresponds to that predicted for a rhombohedral structure.[3,15,16] In our case the band at 256 cm^{-1} can be ascribed to the LiO_6 stretching vibrations, and the absorption bands between 500–700 cm^{-1} can be assigned to vibrations of the $M^{3+}O_6$ octahedral species. In addition, that the spectrum may be divided into two parts suggests the occurrence of distinct LiO_6 and $M^{3+}O_6$ vibrational frequencies,[15,16] which agrees well with the existence of an ordered ion distribution in a distorted rock-salt structure which corresponds to the interpretation of the XRD results.

The SEM image of the $Li_{0.7}Ni_{0.8}Co_{0.2}O_2$ phase (Figure 7) shows the agglomeration of fine particles with a homogeneous particle-size distribution (ca. 1 mμ). It is expected that the particle size should diminish with a shorter reaction time, thus favoring the Li ion diffusivity,[30,39,40] which is very important for rechargeable lithium-ion battery applications.[19,20] However, it has been observed that under such conditions the order in the distribution of the ions, for instance Li^+ and M^{3+} ions, may be not reached. So, to achieve good electrochemical properties it is necessary to establish

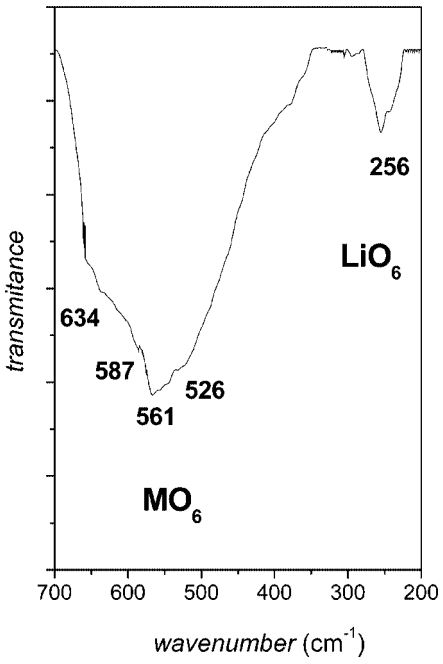

Figure 6. IR spectrum of the $Li_{0.7}Ni_{0.8}Co_{0.2}O_2$ phase obtained after thermal decomposition in air of the $(NH_4)_3LiNi_{0.8}Co_{0.2}(C_6H_5O_7)_2$ citrate precursor at 750 °C for 30 h.

a compromise in the preparation conditions to allow the formation of a well-ordered phase with a relatively small size particle. In the case of the $Li_{0.7}Ni_{0.8}Co_{0.2}O_2$ phase synthesized from the mixed citrate, the particle size is smaller than in the $Li_{0.8}Ni_{0.8}Co_{0.2}O_2$ phase (0.5–20 μm) also obtained in this work by the classical ceramic route. This is also applicable for comparison to other Li-Co-Ni phases obtained from sol-gel precursors followed by calcination at 700–800 °C, such as $LiNi_{0.5}Co_{0.5}O_2$ (3 μm, at 800 °C for 10 h),[9] $LiNi_{0.25}Co_{0.75}O_2$ (1–10 μm at 800 °C for 2 h),[39] and $LiNi_{0.6}Co_{0.4}O_2$ (1 μm, at 700 °C for 4 h).[30]

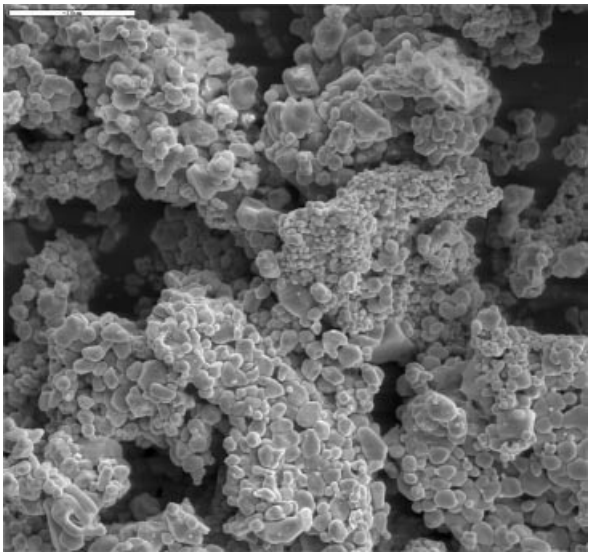

Figure 7. SEM image of the $Li_{0.7}Ni_{0.8}Co_{0.2}O_2$ phase obtained after thermal decomposition in air of the $(NH_4)_3LiNi_{0.8}Co_{0.2}(C_6H_5O_7)_2$ citrate precursor at 750 °C for 30 h.

The study of sample composition carried out by STEM-EDX analysis of different particles shows a high homogeneity in the $Li_{0.7}Ni_{0.8}Co_{0.2}O_2$ phase, with Ni/Co, O/Ni, and O/Co ratios in the 4.09–4.15, 0.70–0.61, and 2.57–2.60 ranges of composition, respectively.

Electrical and Electrochemical Characterization of the $Li_{0.7}Ni_{0.8}Co_{0.2}O_2$ Phase

Figure 8 shows the evolution of the thermoelectric power of the $Li_{0.7}Ni_{0.8}Co_{0.2}O_2$ compound with temperature. All are positive values that are almost independent of the temperature in the studied range. This behavior has been attributed to a small polaron Ni^{3+}-O^{2-}-Ni^{4+}-type transport mechanism, where there is no thermal activation of the number of carriers.[10,40,41] This behavior can be explained by considering the actual lithium content in this sample ($x = 0.7$), hence the loss of the ideal Li^+ stoichiometry may be compensated by the presence of Ni^{4+}/Ni^{3+} couples.[41]

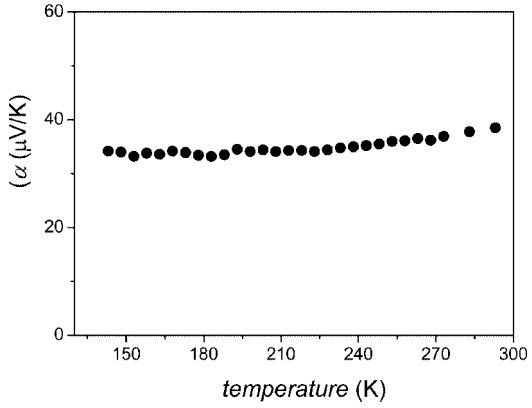

Figure 8. Variation of the thermoelectric power with temperature in the $Li_{0.7}Ni_{0.8}Co_{0.2}O_2$ phase obtained after thermal decomposition in air of the $(NH_4)_3LiNi_{0.8}Co_{0.2}(C_6H_5O_7)_2$ citrate precursor at 750 °C for 30 h.

Previous studies[10,41] have confirmed that, during lithium deintercalation, trivalent nickel ions, rather than trivalent cobalt ions, are preferentially oxidized to the tetravalent state. To unambiguously confirm this behavior a detailed study of the electronic transport properties was carried out during lithium extraction. From a general point of view, nickel oxidation must lead to small polaron-type conductivity, while cobalt oxidation must lead to a tendency to electronic delocalization through the t^2–t^2 overlapping.

Saadoune and Delmas[41] have studied different compositions of $Li_xNi_{0.8}Co_{0.2}O_2$ ($x > 0.5$) and have observed that there is no change in the transport mechanism. Our results for the $Li_{0.7}Ni_{0.8}Co_{0.2}O_2$ phase prepared from the citrate precursor are very similar to theirs and confirm an activated character with an activation energy of 0.17 eV in the electrical conductivity (Figure 9). This result confirms the electronic localization in this phase, which is in good agree-

ment with the presence of Ni^{4+} ions in the material and therefore the existence of Ni^{4+}-O^{2-}-Ni^{3+} hopping. Considering the actual composition of the $Li_{0.7}Ni_{0.8}Co_{0.2}O_2$ phase, it must be assumed that there are a significant number of Ni^{4+} ions, leading to the presence of holes in the Ni^{4+}/Ni^{3+} narrow band and the respective decrease of the Ni^{4+}-O^{2-}-Ni^{3+} distance as a resulting of the higher valence of Ni^{4+}, which makes the Ni^{3+}-O^{2-}-Ni^{4+} hopping easier. Finally, it should be noted that our $Li_{0.7}Ni_{0.8}Co_{0.2}O_2$ presents a good conductivity value in the 10^{-2} S cm^{-1} range, which is one of the requirements for applications in secondary lithium batteries.

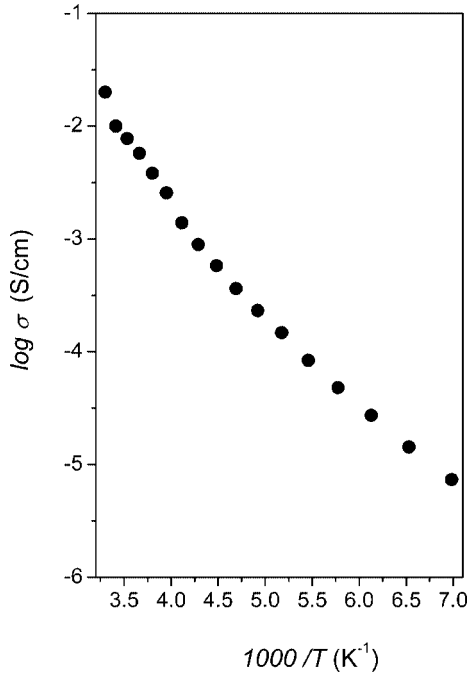

Figure 9. Variation of the electrical conductivity with temperature in the $Li_{0.7}Ni_{0.8}Co_{0.2}O_2$ phase obtained after thermal decomposition in air of the $(NH_4)_3LiNi_{0.8}Co_{0.2}(C_6H_5O_7)_2$ citrate precursor at 750 °C for 30 h.

The first charge and discharge curves of the $Li_{0.7}Ni_{0.8}Co_{0.2}O_2$ phase used as a positive electrode (without any addition of conductive carbon due to its good electrical conductivity) are illustrated in Figure 10, in which the Li content has been varied in the $0.7 \geq x \geq 0.4$ composition domain whilst operating at a 70 μA cm^{-2} current density. This graphic shows that the electrochemical process is well reversible, with the coulombic efficiency of the first discharge process being about 96% of the first charge one. The monotonous increment of the voltage vs. composition curve suggests the occurrence of a monophasic reaction in the charge/discharge process, as has been reported by several authors.[1,7,29,30] On the contrary, for the material obtained by the traditional ceramic method ($Li_{0.8}Ni_{0.8}Co_{0.2}O_2$), the first insertion/deinsertion lithium cycle exhibits a very poor percentage of recovered lithium (about 50%), i.e. a poor reversibility.

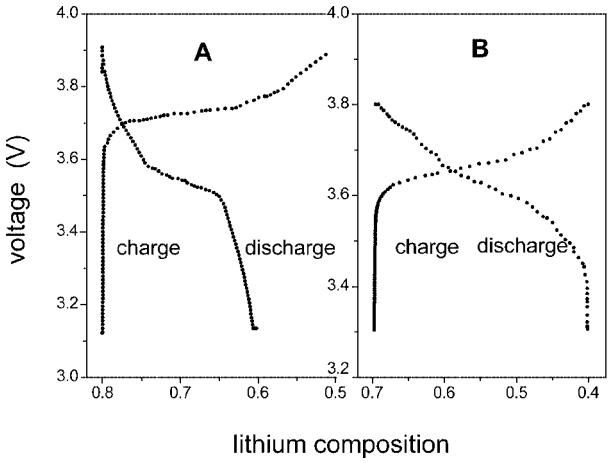

Figure 10. First charge/discharge cycle of (a) the $Li_{0.7}Ni_{0.8}Co_{0.2}O_2$ phase (Li/$LiClO_4$ (PC/EC)/$Li_{0.7}Ni_{0.8}Co_{0.2}O_2$ cell) and (b) the $Li_{0.8}Ni_{0.8}Co_{0.2}O_2$ phase prepared by the ceramic method (Li/$LiClO_4$ (PC/EC)/$Li_{0.8}Ni_{0.8}Co_{0.2}O_2$ cell), both at 70 μA cm^{-2}.

The low polarization effect observed is in good agreement with the lithium content determined from chemical analysis ($x = 0.7$), because it is known that when x becomes close to 1 the ionic conductivity decreases as the number of available sites for Li^+ ion diffusion becomes very small, leading to a strong polarization effect.[41]

Figure 11 shows a plot of the $-dx/dV$ values vs. the potential for the first charge/discharge cycle of the cell prepared from the $Li_{0.7}Ni_{0.8}Co_{0.2}O_2$ phase. The occurrence of a single step of extraction and insertion of lithium from the cathode suggests the existence of a unique phase in our compound, in contrast to the $Li_{0.75}Ni_{0.8}Co_{0.2}O_2$ ceramic phase already reported by Saadone and Delmas.[41] In this last case, the observed minimum in the dx/dV plot is associated with order–disorder transitions during the insertion/deinsertion of the Li^+ ions.

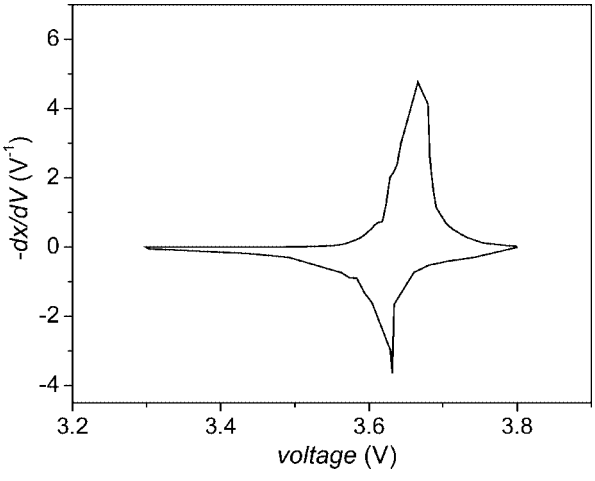

Figure 11. Derivative curve ($-dx/dV$) vs. voltage for the first charge/discharge cycle of the Li/$LiClO_4$(PC/EC)/$Li_{0.7}Ni_{0.8}Co_{0.2}O_2$ cell. In the derivative term, x represents the content of Li.

The excellent cyclability of this cell, at least for the first four charge/discharge processes, is shown in Figure 12. The

data show a specific capacity of 80 mAh g^{-1}, corresponding to the insertion/extraction of 0.3 Li^+. The experimental conditions were selected in order to ensure that the lithium insertion never goes lower than 0.4 moles to avoid irreversible phase transformations. This limitation implies that the maximum amount in the lithium content was that of the starting oxide, i.e. $x = 0.7$.

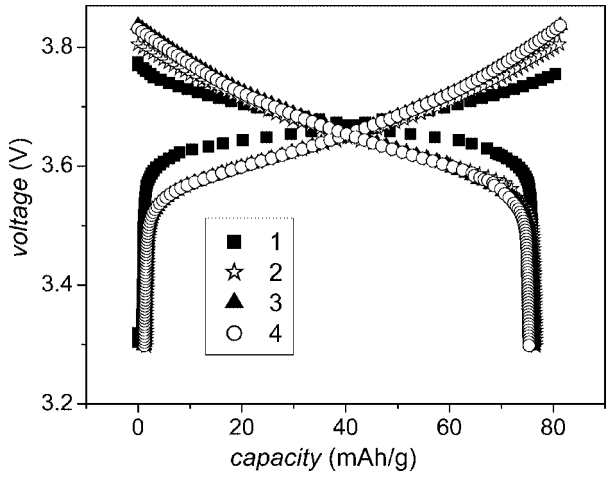

Figure 12. Galvanostatic cycling curves of the Li/$LiClO_4$ (PC/EC)/$Li_{0.7}Ni_{0.8}Co_{0.2}O_2$ cell at a constant current density of 70 μA cm^{-2}. The Li content has been varied in the $0.7 \geq x \geq 0.4$ composition domain.

The theoretical capacity calculated for a variation of $\Delta x = 0.6$ in the lithium content for a similar cell prepared with materials of the same family compounds is about 160 mAh g^{-1},[29,30,41] which is equivalent to the value of 80 mAh g^{-1} obtained by us for $\Delta x = 0.3$ extracted and reinserted.

Concluding Remarks

The main requirement to obtain a Ni-rich phase such as $Li_{0.7}Ni_{0.8}Co_{0.2}O_2$ with well-ordered cationic distribution of Li and Ni from citrate precursors is the pH control in the precursor synthesis to form a unique phase of the mixed citrate. Working at unsuitable pH conditions results in a mixture of citrate phases which, after thermal decomposition, gives rise to mixed oxides presenting a disordered Li/Ni cationic distribution.

The $Li_{0.7}Ni_{0.8}Co_{0.2}O_2$ oxide prepared from the mixed citrate $(NH_4)_3LiNi_{0.8}Co_{0.2}(C_6H_5O_7)_2$ shows good electrical conductivity that is high enough to ensure the required behavior as an electrode material for convenient electrochemical insertion/deinsertion of lithium without addition of conductive carbon.

Comparing the results of electrochemical behavior towards Li insertion/deinsertion of $Li_{0.7}Ni_{0.8}Co_{0.2}O_2$ as an electrode material with that of the already reported $Li_{0.75}Ni_{0.8}Co_{0.2}O_2$ phase prepared by a ceramic method shows that the novel phase presents an enhanced performance in the cyclability properties.

Experimental Section

The Li-Co-Ni citrate with a Li/Co/Ni/citric acid stoichiometry ratio of 1:0.2:0.8:2, respectively, was synthesized by adding Li_2CO_3 (1.92 g; Merck) to a mixture of aqueous solutions of $Co(NO_3)_2 \cdot 6H_2O$ (11.98 g; Riedel-de Haën) and $Ni(NO_3)_2 \cdot 6H_2O$ (2.98 g; Aldrich) to reach the 1:4 Co/Ni stoichiometry selected. A saturated solution of citric acid (Aldrich) was then added dropwise to this mixture, which was stirred rapidly until a clear solution was obtained. Afterwards, the pH was adjusted to 7 with aqueous ammonia (6 M; Merck) and the mixture was heated at 80 °C for 4 h. This thermal treatment produced the formation of a blue-green precipitate, which was isolated, washed with ethanol, and dried at 100 °C in air. The solid was characterized and then used to prepare the mixed oxide by heating at 750 °C for 30 h. For comparative purposes, a $Li_xNi_{0.8}Co_{0.2}O_2$ phase was prepared by a conventional ceramic route based on the thermal decomposition of stoichiometric mixtures of $Ni(NO_3)_2 \cdot 6H_2O$, $Co(NO_3)_2 \cdot 6H_2O$, and $Li(OH) \cdot H_2O$ at 400 °C and subsequent solid-state reaction in air at 750 °C for 30 h.[3]

The elemental analyses (CHN) were performed with a Perkin–Elmer 240C microanalyzer. The Li, Ni, and Co contents were determined with an ICP-AES spectrometer Perkin–Elmer Optima 3300. The mean oxidation state of cobalt and nickel was determined by iodometric titration. The XRD patterns were recorded with a Philips PW1710 diffractometer using Cu-K_α radiation from 10° to 90° (2θ) at 2° min^{-1}. The temperatures for the programmed recording of XRD patterns (5 °C min^{-1}) during the heating of the citrate precursor carried out in the Anton Paar high temperature chamber of the diffractometer, were selected from the DTA and TG curves of the sample obtained in a Seiko SSC/5200 analyzer (5 °C min^{-1} heating rate from room temperature to 900 °C in air). The TG/MS measurement were carried out with a Thermostatar Baltzers Instrument coupled to a Seiko SSC/5200 TG-DTA System using 100 mL min^{-1} He flux, heating from 25 to 600 °C at 2 °C min^{-1}. The Infrared spectra of the citrate precursor (KBr pellets) and mixed oxides (polyethylene pellets) were recorded with an ATI MATTSON Genesis Series FTIR spectrometer in the 400–4000 cm^{-1} region and a Perkin–Elmer FTIR spectrophotometer model 567 in the 200–700 cm^{-1} region, respectively. The morphology, particle-size distribution, and purity of the phases were studied with a SEM Zeiss DSM-960 microscope coupled with an EDX Tacor-Northen Serie Z-II spectrometer operating at 20 kV and a STEM LEO-910 microscope also coupled with an EDX system.

Thermoelectric power and four-point conductivity measurements in the –133 to 20 °C temperature range were carried out simultaneously using a homemade apparatus described elsewhere.[42] Pellets of pressed powder (7 tons cm^{-2}) were sintered at 700 °C for 4 h in air. The electrochemical measurements were carried out in Li/$LiClO_4$(PC/EC)/$Li_xNi_{0.8}Co_{0.2}O_2$ cells. The positive electrode consists of sintered pellets (0.13 cm diameter) pressed at 3 tons cm^{-2} of the pure mixed oxide (i.e., without addition of carbon as electric conductor). The cells, assembled in an argon-filled dry box, were galvanostatically cycled under low current density (70 μA cm^{-2}) in the $0.7 \geq x \geq 0.4$ and $0.8 \geq x \geq 0.4$ lithium composition ranges for the oxides prepared by the chemical and ceramic methods, respectively.

Acknowledgments

Financial support from the CSIC and the Havana University (CITMA) through a Spanish–Cuban cooperation (reference

2001CU0007) and from the CICYT (Spain, MAT2000-1585-C03-01 and MAT2003-06003-C02-01) is gratefully acknowledged. The authors would like to thank Dr. S. Letaïef and Mr. F. Pinto for helpful technical assistance.

[1] J. N. Reimers, J. R. Dahn, *J. Electrochem. Soc.* **1992**, *139*, 2091–2097.
[2] W. Li, J.-N. Reimers, J. R. Dahn, *Solid State Ionics* **1993**, *67*, 123–130.
[3] R. Alcántara, J. Morales, J. L. Tirado, R. Stoyanova, E. Zhecheva, *J. Electrochem. Soc.* **1995**, *142*, 3997–4005.
[4] T. Ohzuku, A. Ueda, *Solid State Ionics* **1994**, *69*, 201–211.
[5] A. Manthiram, J. Kim, *Chem. Mater.* **1998**, *10*, 2895–2909.
[6] M. Broussely, F. Perton, D. Biensan, J. Bodet, A. Lecerf, C. Delmas, A. Rougier, J. P. Pérès, *J. Power Sources.* **1995**, *54*, 109–114.
[7] I. Saadoune, M. Ménétrier, C. Delmas, *J. Mater. Chem.* **1997**, *7*, 2505–2511.
[8] R. J. Gummow, M. M. Tackeray, W. I. David, S. Hull, *Mater. Res. Bull.* **1992**, *27*, 327–337.
[9] D.-W. Kim, Y.-K. Sun, *Solid State Ionics* **1998**, *111*, 243–252.
[10] C. Delmas, I. Saadoune, *Solid State Ionics* **1992**, *53–56*, 370–375.
[11] J. Molenda, P. Wilk, J. Marzec, *Solid State Ionics* **1999**, *119*, 19–22.
[12] A. Rougier, I. Saadoune, P. Gravereau, P. Willman, C. Delmas, *Solid State Ionics* **1996**, *90*, 83–90.
[13] E. Zhecheva, R. Stoyanova, *Solid State Ionics* **1993**, *66*, 143–145.
[14] J. Morales, C. Pérez, J. L. Tirado, *Mater. Res. Bull.* **1990**, *25*, 623–625.
[15] R. K. Moore, W. B. White, *J. Am. Ceram. Soc.* **1970**, *53*, 679–682.
[16] P. Tarte, J. Prudhomme, *Spectrochim. Acta, Ser. A* **1970**, *26A*, 747–754.
[17] R. Stoyanova, E. Zhecheva, R. Alcántara, P. Labela, J. L. Tirado, *Solid State Commun.* **1997**, *102*, 457–462.
[18] J. P. Pérès, C. Delmas, A. Rougier, M. Broussely, F. Perton, P. Biesan, P. Willmann, *J. Phys. Chem. Solids* **1996**, *57*, 1057–1060.
[19] M. Mizushima, P.-C. Jones, P.-J. Wiseman, J.-B. Goodenough, *Solid State Ionics* **1981**, *3/4*, 171–174.
[20] S. Kikkawa, S. Miyazaki, M. Koizumi, *J. Power Sources* **1985**, *14*, 231–234.
[21] D. Heennings, W. Mayr, *Solid State Chem.* **1978**, *26*, 329–338.
[22] D. J. Anderton, F. R. Sale, *Powder Metall.* **1979**, *22*, 14–18.
[23] M. S. Baythoun, F. R. Sale, *J. Mater. Sci.* **1982**, *17*, 2557–2560.
[24] A. Douy, M. Odier, *Mater. Res. Bull.* **1989**, *24*, 1119–1126.
[25] J.-H. Choy, Y.-S. Han, J.-T. Kim, Y.-H. Kim, *J. Mater. Chem.* **1995**, *5*, 57–63.
[26] M. Pechini, *US Patent.* **1967**, 3,330,697.
[27] V. K. Sankaranarayanan, Q. A. Pankhurst, D. P. Disckon, C. E. Johnson, *J. Magn. Magn. Mater.* **1993**, *120*, 73–75.
[28] V. K. Sankaranarayanan, Q. A. Pankhurst, D. P. Disckon, C. E. Johnson, *J. Magn. Magn. Mater.* **1993**, *125*, 199–208.
[29] E. Zhecheva, R. Stoyanova, M. Gorova, R. Alcántara, J. Morales, J. L. Tirado, *Chem. Mater.* **1996**, *8*, 1429–1440.
[30] C. Julien, L. El-Farh, S. Rangan, M. Massot, *J. Sol-Gel Sci. Technol.* **1999**, *15*, 63–72.
[31] *Handbook of Analytical Chemistry* (Ed.: J. Lurie), MIR Publishers, Moscow, **1971**.
[32] R. Swanson, W. H. Ilsey, A. G. Stanislowski, *J. Inorg. Biochem.* **1983**, *18*, 187–194.
[33] R. C. Bott, D. S. Sagatys, D. E. Lynch, G. Smith, C. H. Kennard, T. C. Mak, *Aust. J. Chem.* **1991**, *44*, 1495–1498.
[34] *Infrared and Raman Spectra of Inorganic and Coordination Compounds* (Ed.: K. Nakamoto), John Wiley & Sons, New York, **1986**, pp. 231–282.
[35] J. Catterick, P. Thornton, *Adv. Inorg. Chem. Radiochem.* **1977**, *19*, 291–296.
[36] G. B. Deacon, R. J. Philips, *Coord. Chem. Rev.* **1980**, *33*, 227–231.
[37] L. P. Battaglia, A. B. Corradi, G. Marcotrigiano, L. Menabue, G. C. Pellacanni, *J. Am. Chem. Soc.* **1995**, *117*, 2663–2669.
[38] U. D. Altermatt, I. D. Brown, *Acta Crystallogr. Sect. A* **1987**, *34*, 125–130.
[39] C. C. Chang, N. Scarr, P. N. Kumta, *Solid State Ionics* **1998**, *112*, 329–344.
[40] M. Thackeray, *J. Electrochem. Soc.* **1995**, *142*, 2558–2563.
[41] I. Saadoune, C. Delmas, *J. Solid State Chem.* **1998**, *136*, 8–15.
[42] E. Pérez-Cappe, A. Villanueva, J. C. Gálvan, G. Pérez-Urrutia, E. Ruiz-Hitzky, *Abstracts VI Reunión Nacional de Materiales*, **1999**, San Sebastián.

Received: May 11, 2004
Published Online: May 31, 2005

